New opportunities in interferometric lithography using extreme ultraviolet tabletop lasers

Przemyslaw W. Wachulak
Lukasz Urbanski
Colorado State University
NSF ERC for Extreme Ultraviolet Science & Technology
Department of Electrical and Computer Engineering
Fort Collins, Colorado 80523

Maria G. Capeluto
Universidad de Buenos Aires
Departmento de Fisica
Facultad de Ciencias Exactas y Naturales
Buenos Aires, Argentina

David Hill
Willie S. Rockward
Morehouse College
Department of Physics
Atlanta, Georgia 30314

Claudio Iemmi
Universidad de Buenos Aires
Departmento de Fisica
Facultad de Ciencias Exactas y Naturales
Buenos Aires, Argentina

Erik H. Anderson
Lawrence Berkeley National Laboratory
Berkeley, California

Carmen S. Menoni
Jorge J. Rocca
Mario C. Marconi
Colorado State University
NSF ERC for Extreme Ultraviolet Science & Technology
Department of Electrical and Computer Engineering
Fort Collins, Colorado 80523
E-mail: marconi@engr.colostate.edu

Abstract. The development of tabletop extreme ultraviolet (EUV) lasers opens now the possibility to realize interferometric lithography systems at EUV wavelengths that easily fit on the top of an optical table. The high degree of spatial and temporal coherence and high brightness of the compact EUV laser sources make them a good option for interferometric applications. The combination of these novel sources with interferometric lithography setups brings to the laboratory environment capabilities that so far had been restricted exclusively to large synchrotron facilities.
 [DOI: 10.1117/1.3129837]

Subject terms: nanopatterning; interferometric lithography; extreme ultraviolet (EUV) lasers.

Paper 08153SSRR received Sep. 27, 2008; revised manuscript received Mar. 6, 2009; accepted for publication Mar. 25, 2009; published online May 6, 2009.

1 Introduction

Periodic nanostructures, such as gratings and arrays of holes and pillars, can be used to fabricate UV polarizers, plasmonic structures, highly sensitive detectors based on surface-enhanced Raman scattering, high-density magnetic memories, miniaturized RF oscillators, etc., or to characterize photoresists and lithographic processes.[1–9] Electron beam lithography and focused ion beam lithography provided an excellent method to fabricate these nanostructures with periods below 100 nm. However, due to their intrinsic serial characteristic, they are time consuming and are not well suited for large area patterning. Self-assembly, replication by embossing, molding, or printing with master stamps are also alternatives for large-area nanolithography.[10,11] In the case of self-assembly, the arrangement of nanostructures is frequently organized in reduced areas, while the replication using master stamps needs a different master for each motif, restricting the versatility of the method.

Interferometric lithography (IL) is an attractive and inexpensive alternative for efficient patterning of periodic structures over large areas. The periodic patterns are obtained combining mutually coherent beams at the surface of

1932-5150/2009/$25.00 © 2009 SPIE

a photoresist-coated substrate, creating a sinusoidal profile with a period $d=\lambda/2\sin\theta$, where λ is the wavelength, and θ is the half-angle between the intersecting beams. Also two-dimensional (2-D) motifs can be obtained by combining more than two coherent beams or using multiple exposures.

One approach to reduce the period that can be printed by interference is to use immersion optics to increase the numerical aperture (NA) of the optics.[12] Using short-wavelength lasers or filtered synchrotron radiation for the illumination is the other way to achieve this goal. Savas et al., using an ArF laser ($\lambda=193$ nm) and an achromatic interference setup implemented with phase gratings, demonstrated patterning with periods down to 100 nm.[13,14] Zaidi et al., using multiple exposure, demonstrated patterning of 1-D and 2-D structures with 0.6-μm period.[15]

Further reduction in the period can be achieved utilizing even shorter wavelength radiation from synchrotron facilities. Synchrotrons provide a large photon flux and tunable output, but the spatial and temporal coherence of the beam are much lower than those typically obtained with laser sources. Additional filtering is often necessary to obtain a good contrast in the interference fringes over large areas. This necessary filtering has the immediate consequence of a serious flux reduction. Despite this inconvenience, synchrotrons are always an attractive short-wavelength source for leading-edge IL experiments.

The main advantage of the interferometric lithography scheme is that it provides a relatively simple way to print periodic structures over large areas with a maskless, lensless, noncontact technique. Compact extreme ultraviolet (EUV) laser sources open new possibilities to realize efficient nanopatterning in a compact (tabletop size) setup with similar capabilities to systems now accessible only with synchrotron sources. The development of compact and efficient EUV and soft x-ray lasers facilitated the demonstration of a large number of applications, including lithography, interferometry, microscopy, holography, and nano-ablation.[16–20]

In this paper, we present the development of a compact tabletop nanopatterning tool based on the combination of the well-established interferometric lithography technique and a tabletop EUV laser. In Sec. 2, we present a detailed description of the compact extreme ultraviolet laser sources. Section 3 is devoted to describing a wavefront division interferometric lithography tool based on a Lloyd's mirror interferometer. In Sec. 4, we discuss the results obtained with an amplitude division interferometer implemented with a transmission diffraction grating used as a beamsplitter and two folding mirrors.

2 Compact Tabletop EUV Lasers

The sources utilized in this work are tabletop EUV lasers, as shown in Figs. 1 and 2. This compact EUV laser enabled us to realize in a laboratory environment applications so far restricted to large synchrotron facilities. It is a capillary discharge pumped laser that produces an intense beam at $\lambda=46.9$ nm with the necessary coherence and peak power to realize a robust tabletop nanopatterning tool.

Lasing is obtained in the 46.9-nm 3-s $^1P_1-3p^1S_0$ (J=0 −1) transition of the Ar^{+8} ion (neon-like Ar). An alumina

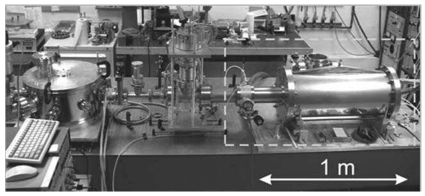

Fig. 1 Tabletop $\lambda=46.9$-nm laser and experiment chamber. The footprint of the system is 2.5×0.75 m^2.

capillary 3.2-mm inner diameter filled with Ar is excited with a current pulse having an amplitude of $\approx$24 kA, a 10% to 90% rise time of $\approx$25 ns, and a first half-cycle duration of $\approx$110 ns. The fast current pulse is produced by discharging a water dielectric cylindrical capacitor through a spark gap switch connected in series with the capillary load. The current pulse rapidly compresses the plasma column to form a dense and hot filamentary plasma channel where population inversion is created between the $3p(^1S_0)$ and $3s(^1P_1)$ levels by strong monopole electron impact excitation of the laser upper level and rapid radiative relaxation of the laser lower level. Water serves as a liquid dielectric for the capacitor and also cools the capillary. A continuous flow of Ar is injected in the front of the capillary, while an optimum Ar gas pressure of 490 mTorr is maintained in the capillary channel.

The tabletop laser produces pulses approximately 400 μJ at repetition rates up to 4 Hz.[21,22] The spatial coherence varies with the length of the gain medium.[23] For a 36-cm-long gain medium, a coherence radius of 550 μm at 1.5 m from the source that includes almost half the entire laser power is obtained. The coherence radius was measured analyzing the fringe visibility of the interference fringes obtained when a mask with two pinholes at different separations was placed at selected distances from the source. The coherence radius R_c characterizes the transverse coherence of the laser beam and was defined following the convention of coherence area used by Goodman.[24] The laser has a narrow spectral bandwidth, $\Delta\lambda/\lambda\leq10^{-4}$, corresponding to a temporal coherence length of 470 μm.

This laser developed at Colorado State University is the highest average power compact coherent EUV source presently available at this wavelength. It is a very compact unit with a footprint of 1×0.5 m^2. Combined with an experi-

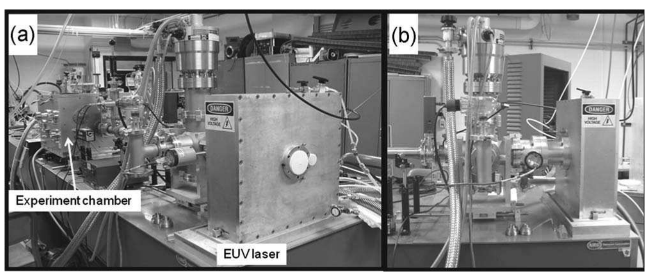

Fig. 2 (a) Photograph of the desktop capillary discharge laser (right) connected using a vacuum manifold to the experiment chamber (left) housing the amplitude division interferometer. (b) Desktop version of the capillary discharge laser with an energy per pulse about 10 μJ and a repetition rate up to 12 Hz.

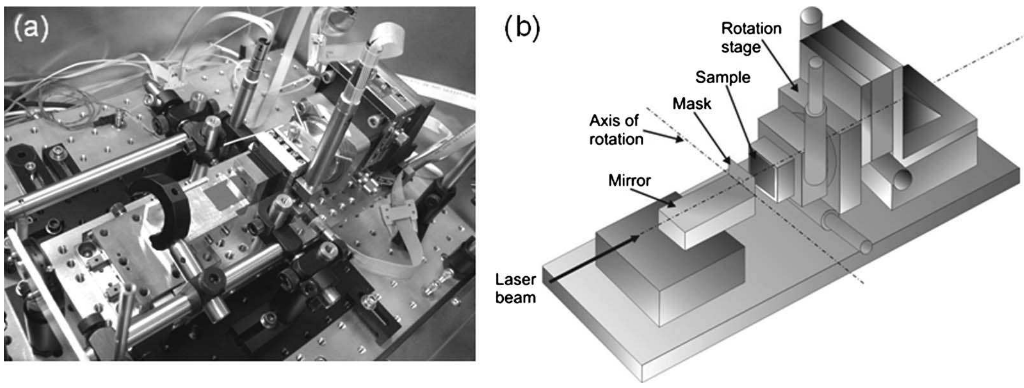

Fig. 3 Wavefront division interferometer based on a Lloyd's mirror. The setup allows for multiple exposures of the sample with arbitrary rotation angles around an axis parallel to the mirror's surface.

ment chamber, the system easily fits on top of an optical table. Figure 1 shows the laser and the experiment chamber.

A more compact version of the EUV laser was used in combination with an amplitude division interferometer (ADI) that will be described in Sec. 4. Figure 2 shows this more compact, "desktop" size EUV laser. The desktop $\lambda = 46.9$-nm Ne-like Ar capillary discharge laser emits pulses with lower energy, approximately 10 μJ at repetition rates up to 12 Hz (Ref. 25).

3 Wavefront Division Interferometric Lithography

In wavefront division interferometers, the interfering beams are obtained by dividing the incoming wavefront into two or more beams. One example is the multiple beams scheme generated using a mask composed of several diffraction gratings arranged in different configurations. This mask allows for great versatility in the shape, period, and configuration of the arrays of structures. By changing the orientation, period, and number of the gratings, it is possible to print arrays of holes in square or circular patterns.[26–30] Another attractive wavefront division scheme is the Lloyd's mirror interferometer. Because of its simplicity, it is a convenient configuration for IL at EUV wavelengths. With this scheme, Solak et al. demonstrated 19-nm line and space gratings (38-nm period) in polymethyl methacrylate (PMMA) photoresist with 13.4-nm wavelength illumination.[31,32]

Using a Lloyd's mirror scheme combined with multiple exposures, we were able to print different 2-D motifs. Figure 3 shows a scheme and a picture of the actual device. The sample is mounted in a rotation stage to allow arbitrary angle rotations around an axis parallel to the mirror's surface. All the critical movements are controlled by vacuum compatible actuators that allow multiple exposures *in situ* with identical experimental conditions. Figure 4 shows atomic force microscope micrographs of different patterns obtained in PMMA with different rotation angles α between the two exposures. With $\alpha = \pi/2$, symmetric dots are obtained, as shown in Fig. 4(a). If the rotation angle is changed to $\alpha = \pi/6$, regular elongated dots are produced instead, as shown in Fig. 4(b).

Changing the exposure dose allows for the fabrication of pillars or holes. This can be understood in the following way. With a small dose, the PMMA is activated only in thin lines corresponding to the interference maxima. The superposition of two exposures develops small holes in the loci where the maxima of interference superpose. On the other hand, if the dose is increased, the PMMA is activated in wide trenches, developing in the intersection of the minima small regions with unexposed photoresist that resembled cone-shaped nanodots.[19] The height of the features printed in PMMA is 25 to 30 nm, limited by the penetration depth of the EUV photons in this resist.

An alternative to increasing the height of the structures is to use the Si-based photoresist hydrogen silsesquioxane (HSQ). The 46.9-nm photons from the EUV laser have a larger penetration depth in this photoresist, in excess of 120 nm. Figure 5 shows an example of the structures that can be fabricated. Figure 5(a) shows an atomic force micrograph of an array of dots obtained with a low exposure dose. The HSQ is activated in small volumes corresponding to the maxima of intensity, creating symmetric dots. If the dose is increased, a regular array of holes is obtained instead, about 130-nm FWHM and 120-nm depth, as shown in Fig. 5(b). For higher doses, the photoresist is activated in wide strips along the maxima of interference, which develops symmetric holes in the loci where the minima of interference superpose.

The Lloyd's mirror configuration combined with the tabletop EUV laser constitutes a simple and versatile inter-

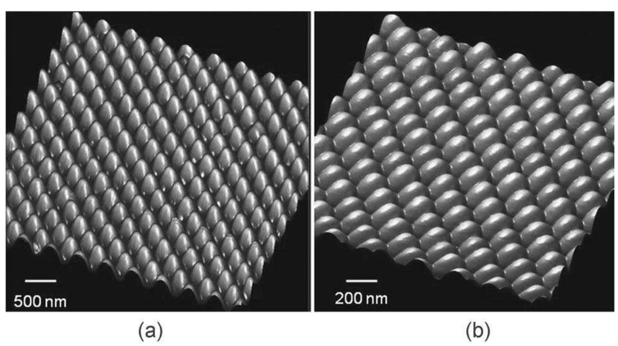

Fig. 4 Arrays of symmetric (a) and elongated (b) nanodots printed in PMMA using a Lloyd's mirror interferometer with two successive exposures after rotating the sample by an angle $\alpha = \pi/2$ and $\alpha = \pi/6$, respectively.

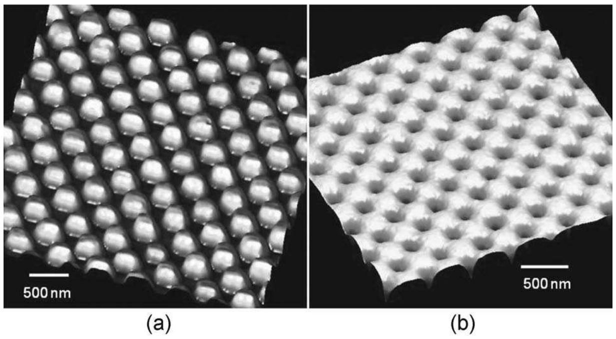

Fig. 5 (a) Dots and (b) holes fabricated in HSQ with a Lloyd's mirror interferometer and two successive exposures. The change from dots to holes is obtained by changing the exposure dose. The FWHM of the holes is 130 nm, and the depth is 120 nm.

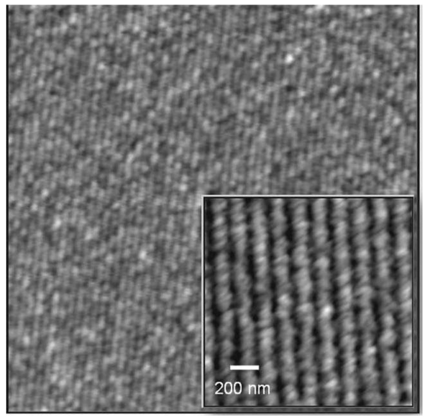

Fig. 7 Atomic force microscope scan of a 145-nm-period grating printed on HSQ using an amplitude division interferometer.

ferometric tool capable of producing various features with minimal changes in the exposure conditions. All the patterns shown in Figs. 4 and 5 were obtained with typical exposure times of 1 to 2 min. The printed area is limited to $500 \times 500\ \mu m^2$ by the spatial coherence of the laser source. This limitation can be overcome utilizing an amplitude division interferomer, which will be described in the next section.

4 Amplitude Division Interferometric Lithography

To obtain high-contrast fringes in a wavefront division scheme, the interfering beams must be mutually coherent, and that requirement imposes the necessity of a highly spatial coherent illumination. In an amplitude division scheme, this requirement is more relaxed because the interference is obtained by the superposition of two beams that are replicas of the original wavefront. This scheme allows "achromatic" interferometric lithography, where temporal coherence is not relevant and spatial coherence limits the depth of focus of the system.[33]

To overcome the limitations on the printable area imposed by the spatial coherence of the laser in the wavefront division interferometer, we developed an amplitude division interferometer (ADI) IL system. The ADI is based on a transmission diffraction grating used as a beamsplitter and two folding mirrors. The grating was fabricated by electron beam lithography in a thick ($1\ \mu m$) photoresist layer supported on a 100-nm-thick Si membrane. A scheme and a photograph of the device are shown in Fig. 6.

The transmission diffraction grating splits the illuminating laser beam into two beams corresponding to the two first diffraction orders. The two beams are recombined in the surface of the sample after the reflection in two grazing mirrors implemented with Si wafers. When illuminated with a collimated beam, the grating produces two replicas of the wavefront that are mutually coherent. The requirement for this configuration is to superpose the two beams in the sample with an accuracy better than the transverse coherence length of the laser; which for our experimental conditions is a fraction of a millimeter.[23] The optical path difference between the two interferometer branches has to be adjusted better than the longitudinal coherence, approximately 0.5 mm.

Figure 7 shows a line grating pattern with a period of 145 nm (72.5-nm-thick lines) printed on HSQ with the ADI setup. The printed area is $2 \times 0.6\ mm^2$, corresponding to the size of the diffraction grating used as a beamsplitter. Gratings with smaller period, down to 95 nm, were also printed, increasing the angle between the two beams im-

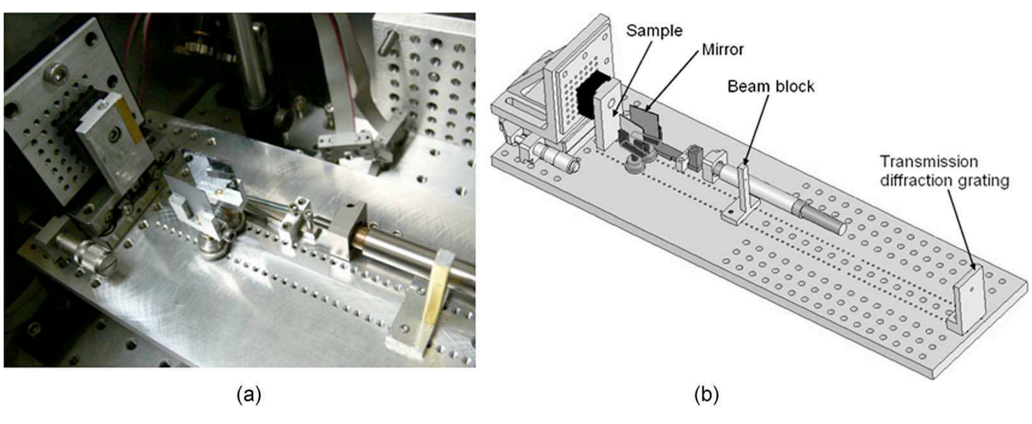

Fig. 6 Amplitude division interferometric lithography setup. The laser beam is split using a transmission diffraction grating into two beams corresponding to the two first diffraction orders. The two beams are recombined in the sample surface on reflections in two grazing mirrors.

pinging at the sample. However, the 95-nm-period gratings showed an increased noise and lower modulation as compared to the larger period gratings.

The lower quality of the gratings printed with this interferometer can be understood if we consider that for this experiment, we used the smaller version (desktop) laser, which provides a substantially lower energy per pulse (about 10 μJ per pulse). This lower photon flux increased the necessary exposure times to approximately 10 min. The increased exposure time might be an explanation for this lower quality printing because vibrations during the exposure play a more important role. In addition, the print quality may possibly be affected by photoresist scumming, which is particularly severe in 50% duty cycle lines with line widths approaching 50 nm (Ref. 34). The quality of the beamsplitter grating and the folding mirrors is also a possible reason for the increased noise in the gratings printed with this interferometer. The presence of scattering centers in the grating and mirrors might introduce a random noise background, reducing the fringe visibility and the quality of the patterns. Furthermore, small variations in the thickness of the Si membrane that supports the transmission grating can introduce random phase and intensity variations across the beam that also reduces the fringe visibility.

5 Summary

In summary, we presented a compact EUV interferometric lithography tool that combines compact EUV lasers with wavefront division and amplitude division interferometers to realize tabletop nanopatterning test beds. With the wavefront division scheme, lines and 2-D structures were printed with exposure times of a few minutes over surfaces of the order of a fraction of one millimeter square. By changing the experimental conditions, it was possible to modify the patterns from pillars to holes or to print symmetric or elongated features with feature size down to 60 nm. Using an amplitude division scheme, lines with periods down to 95 nm were obtained. For this interferometer however, the quality of the beamsplitter must be improved to increase the line modulation of the printed gratings.

The continuing development of tabletop laser-excited EUV lasers capable of emitting in the region below 20 nm in combination with these interferometric lithography tools can potentially further reduce the periods of the printed structures. The shorter wavelength lasers are obtained by irradiating a solid target with a short high-energy laser pulse to produce an elongated plasma column were strong gain is obtained in the $4d^1S_0$-$4p^1P_1$ transition of Ni-like ions in Ru, Pd, Ag, Cd, Sn, Sb, and Te (Ref. 35). Recently, the possibility of enhancing the beam spatial coherence by seeding the plasma amplifiers with short high-harmonic pulses was also demonstrated.[36] These capabilities would enable the demonstration of practical EUV IL tools for the quick fabrication of large arrays of periodic features in research-oriented prototyping that so far were restricted to the use of large synchrotron facilities.

Acknowledgments

This work was supported by the NSF ERC for Extreme Ultraviolet Science and Technology, Award No. EEC-0310717 and by supplemental funding for collaborative research with Morehouse College. M.G.C. acknowledges support through a fellowship from CONICET. C.I. acknowledges support from UBA and CONICET.

References

1. V. Pelletier, K. Asakawa, M. S. Wu, D. H. Adamson, R. A. Register, and P. M. Chaikin, “Aluminum nanowire polarizing grids: fabrication and analysis,” *Appl. Phys. Lett.* **88**, 211114 (2006).
2. E. E. Scime, E. H. Anderson, D. J. McComas, and M. L. Schattenburg, “Extreme ultraviolet polarization and filtering with gold transmission gratings,” *Appl. Opt.* **34**, 648–654 (1995).
3. H. Ko, S. Singamaneni, and V. V. Tsukruk, “Nanostructured surfaces and assemblies as SERS media,” *Small* **4**, 1576–1599 (2008).
4. P. R. Krauss and S. Y. Chou, “Nano-compact disks with 400 Gbit/in^2 storage density fabricated using nanoimprint lithography and read with proximal probe,” *Appl. Phys. Lett.* **71**, 3174–3176 (1997).
5. S. Y. Chou and P. R. Krauss, “65 Gbits/in^2 quantum magnetic disk,” *J. Appl. Phys.* **79**, 5066–5066 (1996).
6. M. Moskovits, “Surface-enhanced spectroscopy,” *Rev. Mod. Phys.* **57**, 783–826 (1985).
7. S. Kaka, M. R. Pufall, W. H. Rippard, T. J. Silva, S. E. Russek, and J. A. Katine, “Mutual phase-locking of microwave spin torque nano-oscillators,” *Nature (London)* **437**, 389–392 (2005).
8. F. B. Mancoff, N. D. Rizzo, B. N. Engel, and S. Tehrani, “Phase-locking in double-point-contact spin-transfer devices,” *Nature (London)* **437**, 393–395 (2005).
9. W. Hinsberg, F. A. Houle, J. Hoffnagle, M. Sanchez, G. Wallraff, M. Morrison, and S. Frank, “Deep-ultraviolet interferometric lithography as a tool for assessment of chemically amplified photoresist performance,” *J. Vac. Sci. Technol. B* **16**, 3689–3694 (1998).
10. S. Y. Chou, P. R. Krauss, and P. J. Renstrom, “Nanoimprint lithography,” *J. Vac. Sci. Technol. B* **14**, 4129–4133 (1996).
11. S. O. Kim, H. H. Solak, M. P. Stoykovich, N. J. Ferrier, J. J. de Pablo, and P. F. Nealey, “Epitaxial self-assembly of block copolymers on lithographically defined nanopatterned substrates,” *Nature (London)* **424**, 411–414 (2003).
12. S. R. J. Brueck, “Optical and interferometric lithography—nanotechnology enablers,” *Proc. IEEE* **93**, 1704–1721 (2005).
13. T. A. Savas, M. L. Schattenburg, J. M. Carter, and H. I. Smith, “Large-area achromatic interferometric lithography for 100-nm period gratings and grids,” *J. Vac. Sci. Technol. B* **14**, 4167–4170 (1996).
14. T. A. Savas, S. N. Shah, M. L. Schattenburg, J. M. Carter, and H. I. Smith, “Achromatic interferometric lithography for 100-nm-period gratings and grids,” *J. Vac. Sci. Technol. B* **13**, 2732–2735 (1995).
15. S. H. Zaidi and S. R. J. Brueck, “Multiple exposure interferometric lithography,” *J. Vac. Sci. Technol. B* **11**, 658–666 (1993).
16. J. Filevich, M. C. Marconi, K. Kanizay, J. L. A. Chilla, and J. J. Rocca, “Dense plasma interferometry with a tabletop soft x-ray laser and an amplitude division interferometer based on diffraction gratings,” *J. Phys. IV* **11**, 483–486 (2001).
17. G. Vaschenko, E. Brizuela, C. Brewer, M. Grisham, H. Mancini, C. S. Menoni, M. C. Marconi, J. J. Rocca, W. Chao, J. A. Liddle, E. H. Anderson, D. T. Attwood, A. V. Vinogradov, I. A. Artioukov, Y. P. Pershyn, and V. V. Kondratenko, “Nanoimaging with a compact extreme-ultraviolet laser,” *Opt. Lett.* **30**, 2095–2097 (2005).
18. G. Vaschenko, A. G. Etxarri, C. S. Menoni, J. J. Rocca, O. Hemberg, S. Bloom, W. Chao, E. H. Anderson, D. T. Attwood, Y. Lu, and B. Parkinson, “Nanometer-scale ablation with a tabletop soft x-ray laser,” *Opt. Lett.* **31**, 3615–3617 (2006).
19. P. W. Wachulak, M. G. Capeluto, M. C. Marconi, C. S. Menoni, and J. J. Rocca, “Patterning of nano-scale arrays by tabletop extreme ultraviolet laser interferometric lithography,” *Opt. Express* **15**, 3465–3469 (2007).
20. P. W. Wachulak, M. C. Marconi, R. A. Bartels, C. S. Menoni, and J. J. Rocca, “Soft x-ray laser holography with wavelength resolution,” *J. Opt. Soc. Am. B* **25**, 1811–1814 (2008).
21. B. R. Benware, C. H. Moreno, D. J. Burd, and J. J. Rocca, “Operation and output pulse characteristics of an extremely compact capillary-discharge tabletop soft-x-ray laser,” *Opt. Lett.* **22**, 796–798 (1997).
22. C. D. Macchietto, B. R. Benware, and J. J. Rocca, “Generation of millijoule-level soft-x-ray laser pulses at a 4-Hz repetition rate in a highly saturated tabletop capillary discharge amplifier,” *Opt. Lett.* **24**, 1115–1117 (1999).
23. Y. Liu, M. Seminario, F. G. Tomasel, C. Chang, J. J. Rocca, and D. T. Attwood, “Achievement of essentially full spatial coherence in a high-average-power soft-x-ray laser,” *Phys. Rev. A* **6303**, 033802 (2001).
24. J. W. Goodman, *Statistical Optics*, Wiley, New York (1985).

25. S. Heinbuch, M. Grisham, D. Martz, and J. J. Rocca, "Demonstration of a desktop size high repetition rate soft x-ray laser," *Opt. Express* **13**, 4050–4055 (2005).
26. H. H. Solak, "Space-invariant multiple-beam achromatic EUV interference lithography," *Microelectron. Eng.* **78–79**, 410–416 (2005).
27. H. H. Solak, "Nanolithography with coherent extreme ultraviolet light," *J. Phys. D* **39**, R171–R188 (2006).
28. H. H. Solak and C. David, "Patterning of circular structure arrays with interference lithography," *J. Vac. Sci. Technol. B* **21**, 2883–2887 (2003).
29. H. H. Solak, C. David, J. Gobrecht, L. Wang, and F. Cerrina, "Multiple-beam interference lithography with electron beam written gratings," *J. Vac. Sci. Technol. B* **20**, 2844–2848 (2002).
30. A. Fernandez, J. Y. Decker, S. M. Herman, D. W. Phillion, D. W. Sweeney, and M. D. Perry, "Methods for fabricating arrays of holes using interference lithography," *J. Vac. Sci. Technol. B* **15**, 2439–2443 (1997).
31. H. H. Solak, D. He, W. Li, and F. Cerrina, "Nanolithography using extreme ultraviolet lithography interferometry: 19 nm lines and spaces," *J. Vac. Sci. Technol. B* **17**, 3052–3057 (1999).
32. H. H. Solak, D. He, W. Li, S. Singh-Gasson, F. Cerrina, B. H. Sohn, X. M. Yang, and P. Nealey, "Exposure of 38-nm-period grating patterns with extreme ultraviolet interferometric lithography," *Appl. Phys. Lett.* **75**, 2328–2330 (1999).
33. A. Yen, E. H. Anderson, R. A. Ghanbari, M. L. Schattenburg, and H. I. Smith, "Achromatic holographic configuration for 100-nm-period lithography," *Appl. Opt.* **31**, 4540–4545 (1992).
34. D. P. Mancini, K. A. Gehoski, E. Ainley, K. J. Nordquist, D. J. Resnick, T. C. Bailey, S. V. Sreenivasan, J. G. Ekerdt, and C. G. Willson, "Hydrogen silsesquioxane for direct electron-beam patterning of step and flash imprint lithography templates," *J. Vac. Sci. Technol. B* **20**, 2896–2901 (2002).
35. Y. Wang, M. A. Larotonda, B. M. Luther, D. Alessi, M. Berrill, V. N. Shlyaptsev, and J. J. Rocca, "Demonstration of high-repetition-rate tabletop soft-x-ray lasers with saturated output at wavelengths down to 13.9 nm and gain down to 10.9 nm," *Phys. Rev. A* **72**, 053807 (2005).
36. Y. Wang, E. Granados, F. Pedaci, D. Alessi, B. Luther, M. Berrill, and J. J. Rocca, "Phase-coherent, injection-seeded, tabletop soft-x-ray lasers at 18.9 nm and 13.9 nm," *Nature Photon.* **2**, 94–98 (2008).

Przemyslaw W. Wachulak received an MS degree in optoelectronics at the Electrical and Computer Engineering Department, Military University of Technology, Warsaw, in 2004. Currently, he is working toward a PhD degree at the National Science Foundation (NSF) Engineering Research Center for EUV Science and Technology, Colorado State University. His doctoral research concerns EUV technology, especially high-resolution holography and new approaches to nanopatterning.

Lukasz Urbanski received his master's degree in electrical and computer engineering from the Military University of Technology in Warsaw. Currently, he is studying for his doctoral degree at the National Science Foundation (NSF) Engineering Research Center for EUV Science and Technology, Colorado State University. The area of his research is application of EUV compact tabletop laser sources to nanopatterning and interferometric lithography.

Maria G. Capeluto received the Licenciado diploma in physics in 2002 from the University of Buenos Aires, Argentina. Her research interests include two-photon absorption fluorescence microscopy and the development of nanopatterning techniques using tabletop EUV lasers. She is currently working toward her PhD degree, studying new approaches to nanopatterning.

David Hill is currently a junior physics major with a minor in mathematics at Morehouse College in Atlanta, Georgia. He participated in the REU Program at Colorado State University, where he conducted research on interferometric lithography. Upon graduation from Morehouse, he plans to pursue a PhD in electrical engineering.

Willie S. Rockward is currently an associate professor in the Department of Physics and the director of the Micro/Nano Optics Research and Engineering (MORE) Laboratory at Morehouse College. His current research interests include micro/nano optics lithography, extreme ultraviolet interferometry, optical quadrature microscopy, terahertz imaging, nanostructure characterization, and crossed phase optics. Dr. Rockward is a member of the OSA, IEEE, NSBP, SPS, and AAPT.

Claudio Iemmi received his MSc and PhD degrees in physics from the Universidad de Buenos Aires, Argentina, in 1984 and 1988, respectively. His research interests include optical signal processing, spatial light modulators, optical pattern recognition, and interferometry. He is currently a professor of physics with the Universidad de Buenos Aires and a member of the research staff of Consejo Nacional de Investigaciones Cientificas y Técnicas of Argentina.

Erik H. Anderson attended the Massachusetts Institute of Technology in Cambridge, Massachusetts, and received his BS in 1981, MS in 1984, and PhD in 1988, all from the Department of Electrical Engineering and Computer Science. He joined Lawrence Berkeley National Laboratory in 1988 and worked as a visiting scientist at the IBM T.J. Watson Research Laboratory in Yorktown Heights, New York, developing zone plate optics for x-ray microscopy. In 1993, he moved to Berkeley to build and managed the nanofabrication facility within the Center for X-Ray Optics. From 2001 to 2005, he was the director of the Center for X-Ray Optics. He is currently involved in EUV and soft x-ray optics development, characterization, nanofabrication, and x-ray microscopy.

Carmen S. Menoni received her PhD in physics from Colorado State University (CSU) in 1987. Since 1991, she has been a member of the faculty in the Department of Electrical and Computer Engineering at CSU, where she is presently a professor. Professor Menoni's research bridges optical to material science. Her interests include the use of bright coherent beams of light of wavelengths between 10 to 50 nm for applications such as imaging and ablation. She is also engaged in the growth and characterization of oxide materials for the engineering of interference coatings for high-power lasers.

Jorge J. Rocca is a University Distinguished Professor in the Departments of Electrical and Computer Engineering and of Physics at Colorado State University. He serves as the director of the National Science Foundation Engineering Research Center for Extreme Ultraviolet Science and Technology, a collaboration with the University of Colorado and the University of California, Berkeley. His research interests are in the development, physics, and applications of compact soft x-ray lasers. He has published more than 190 peer review journal article on these topics. Professor Rocca is a fellow of the APS, OSA, and IEEE. He has served as an associate editor of *IEEE Journal of Quantum Electronics*, guest editor of *IEEE Journal of Selected Topics in Quantum Electronics*, and a member of the editorial board of the *Review of Scientific Instruments*. He was elected IEEE LEOS Distinguished Lecturer for 2006 to 2007 and was an NSF Presidential Young Investigator.

Mario C. Marconi is currently a professor in the Electrical and Computer Engineering Department at Colorado State University. As a participating faculty in the NSF ERC for Extreme Ultraviolet Science and Technology, his interests include the development of tabletop EUV lasers and the applications of EUV coherent sources in nanopatterning, interferometry, and high-resolution imaging. Dr. Marconi is a member of the OSA, IEEE-LEOS, and APS.